Research article

Journal of Molecular Recognition

Received: 11 June 2015, Revised: 25 November 2015, Accepted: 4 December 2015, Published online in Wiley Online Library: 21 January 2016

(wileyonlinelibrary.com) DOI: 10.1002/jmr.2531

Tuning FRET efficiency as a novel approach for improved detection of naphthalene: application to environmental samples

Sandip Nandi[a], Sangita Adhikari[a], Sandip Mandal[a], Arnab Banerjee[b]** and Debasis Das[a]*

Naphthalene has emission in the ultraviolet (UV) region, limiting its trace level determination in biological and environmental samples due to detrimental effect of UV light on the living cell and interference from other substances having emission in the UV region. Fluorescence resonance energy transfer strategy is adopted for determination of traces naphthalene in the visible region. Significant improvement of lowest detection limit of naphthalene has been achieved through tuning of fluorescence resonance energy transfer efficiency. Anthranilic acid pyrene (ANP) conjugate provides lowest detection limit for naphthalene among three probes studied, viz. ANB, aniline- pyrene conjugate (APA) and ANP. ANP efficiently measures naphthalene content in river water. Copyright © 2016 John Wiley & Sons, Ltd.
Additional supporting information may be found in the online version of this article at the publisher's web site.

Keywords: FRET; naphthalene; anthranilic acid; pyrene

INTRODUCTION

Polycyclic aromatic hydrocarbons (PAHs) fall within the 10 most toxic classes of compounds, categorized by Centre for Disease Control in 2011 (Serio *et al*., 2013). Naphthalene, the smallest member of PAH family, widely used as moth repellent for clothes or blankets sublimes easily into the atmosphere. Hence, contamination of naphthalene in environment, viz. air, food and water, has become a serious problem. It damages red blood cells and causes nausea, vomiting, diarrhoea and blood excretion in urine. It also causes cataracts causing cloudy vision to animals contaminated by naphthalene via food and breath (Agency for Toxic Substances and Disease Registry, ATSDR, 1996; U.S. Environmental Protection Agency, 1994). Aqueous solubility is a fundamental parameter in evaluating the toxicity of PAHs as it allows spreading over the living systems making contamination easier. Because of higher water solubility of naphthalene over other PAHs, its trace level detection and estimation is important. Methods for naphthalene determination are mainly based on high-performance liquid chromatography (Diaz *et al*., 1999; Kishikawa *et al*., 2003; Gautam *et al*., 2011) or other chromatography techniques (Hossain *et al*., 2014; Andreoli *et al*., 1999). Fluorescence method has several advantages over chromatographic detection such as easy sample preparation protocols, convenient operation, fast response, low cost and high sensitivity (Zhu *et al*., 2010; Han *et al*., 2012; Anbu *et al*., 2012).To the best of our knowledge, fluorescence probe for selective trace level determination of naphthalene is not reported yet. Presently, our research focuses to develop fluorescence probes selective for cations (Banerjee *et al*., 2012; Sahana *et al*., 2011; Das *et al*., 2013) anions (Banerjee *et al*., 2013a; Sahana *et al*., 2012; Lohar *et al*., 2013), amino acids (Das *et al*., 2011; Banerjee *et al*., 2013b) and small molecules. Naphthalene has emission at ultraviolet region, making difficult for its fluorescence determination. Our aim is to develop a strategy that shifts naphthalene emission to visible region. Several photo sensing processes, viz. photo-induced electron transfer (Kim and Quang, 2007; Aoki *et al*., 1992; Ji *et al*., 1999; Leray *et al*., 1999; Leray *et al*., 2001), intermolecular charge transfer (Xu *et al*., 2005; Wang *et al*., 2006), chelation-enhanced fluorescence (CHEF) (Lim *et al*., 2005; Guha *et al*., 2012; Das *et al*., 2012), excimer/exciplex formation (Weller, 1956) and fluorescence resonance energy transfer (FRET) (Förster, 1948; Förster, 1949; van der Meer *et al*. 1994), are available for selective determination of the analytes. Herein, we have synthesized three new fluorescence probes (ANP, APA and ANB) based on pyrene/anthranilic acid as FRET acceptor whereas naphthalene functions as donor. All three probes are able to shift naphthalene emission into visible region. Anthranilic acid, chosen for water solubility, in conjugation with another aromatic ring, behaves as a good FRET acceptor. Pyrene is chosen for its π-stacking ability with naphthalene. The lowest detection of limit (LOD) for naphthalene is significantly improved by tuning the FRET efficiency via changing the acceptor to pyrene-anthranilic acid conjugate. Finally, Gomti river water (India) is analysed to determine the naphthalene content (Malik *et al*. 2011).

* *Correspondence to: D. Das, Department of Chemistry, The University of Burdwan, Golapbag, Burdwan, India.*
E-mail: ddas100in@yahoo.com
** *A. Banerjee, Department of Chemistry & Biochemistry, The University of Texas at Austin, Austin, TX, USA.*
E-mail: ab.bur@utexas.edu

a *S. Nandi, S. Adhikari, S. Mandal, D. Das*
Department of Chemistry, The University of Burdwan, Golapbag, Burdwan, India

b *A. Banerjee*
Department of Chemistry & Biochemistry, The University of Texas at Austin, AustinTX, USA

EXPERIMENTAL

Materials and methods

Pyrene-1-carboxaldehyde, anthranilic acid, benzaldehyde and aniline have been purchased from Sigma Aldrich (India). Spectroscopic grade solvents have been used. Other chemicals are of analytical reagent grade and used without further purification. Mili-Q 18.2 MΩ cm^{-1} water has been used throughout all the experiments. A Shimadzu Multi Spec 1501 spectrophotometer is used for recording ultraviolet–Vis spectra. Fourier transform infrared (FTIR) spectra are recorded on a PerkinElmer FTIR (model RX1, USA) spectrophotometer. Mass spectra are obtained using QTOF Micro YA 263 mass spectrometer in ES positive mode. Proton nuclear magnetic resonance (^{1}H NMR) spectra have been recorded using Bruker Avance 400 (400 MHz) instrument in dimethyl sulfoxide (DMSO)-d_6. Time-resolved fluorescence life-time measurements were performed using a picosecond pulsed diode laser-based time-correlated single photon counting spectrometer from IBH (London, UK) at λ_{ex} = 280 nm and Microchannel Plate Photomultiplier Tubes (MCP-PMT) as a detector. The emission from the sample was collected at a right angle to the direction of the excitation beam maintaining magic angle polarization (54.71). The full width at half maximum of the instrument response function was 250 ps, and the resolution was 28 ps per channel. The data were fitted to multiexponential functions after deconvolution of the instrument response function by an iterative reconvolution technique using IBH DAS 6.2 data analysis software in which reduced w2 and weighted residuals serve as parameters for goodness of fit.

Synthesis of 2-((pyren-1-ylmethylene) amino) benzoic acid (ANP) (Scheme 1)

A 0.050 g Anthranilic acid (0.365 mmol) was dissolved in methanol. To this solution, pyrene-1-carboxaldehyde (0.084 g, 0.365 mmol) was added and refluxed under atmospheric pressure at 80 °C for 4 h. The red coloured reaction mixture was cooled under room temperature, and the clear solution was kept for 2 days. The solid product obtained was recrystallized from methanol with 75% yield. The product was characterized by: ^{1}H NMR (Figure S1) (400 MHz, DMSO-d_6) δ (ppm): 6.47 (1H, d, J = 8.0 Hz), 6.71 (1H, d, J = 10.0 Hz), 7.19 (1H, t, J = 7.2 Hz), 7.66 (1H, d, J = 8.8 Hz), 8.18 (1H, m), 8.29 (1H, m), 8.42 (2H, m), 8.47 (4H, m), 8.57 (1H, m), 9.37 (1H, s), 10.81 (1H, s). QTOF-MS ES^+ (Figure S2), m/z $(M+H)^+$, calculated for $C_{24}H_{16}NO_2$: 350.1176, found, 350.1288. FTIR (neat) (Figure S3) ν_{max} = 1587 and 1708 cm^{-1}.

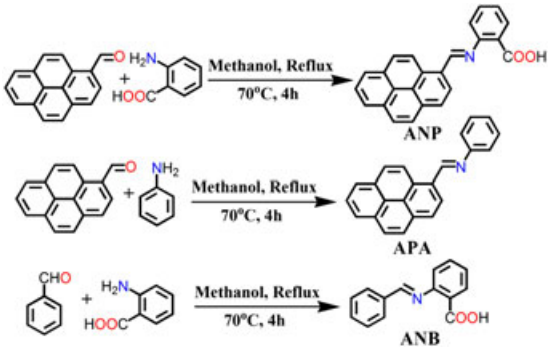

Scheme 1. Synthesis of the probes.

Synthesis of *N*-phenyl-1-(pyren-1-yl) methanamine (APA) (Scheme 1)

To the methanol solution of aniline (0.034 g, 0.365 mmol), pyrene-1-carboxaldehyde (0.084 g, 0.365 mmol) was dissolved and refluxed under atmospheric pressure at 80 °C for 4 h. A dark yellow coloured reaction mixture was obtained and cooled under room temperature, and a solid product was obtained after 2 days. The residue was recrystallized from methanol Yield, 80 %. The product was characterized by: ^{1}H NMR (Figure S4) (400 MHz, DMSO-d_6) δ (ppm): 7.33 (1H, t, J = 8.8), 7.51 (4H, m), 8.17 (1H, d, J = 7.6), 8.25 (1H, d, J = 9.2), 8.31 (1H, d, J = 8.8), 8.39 (1H, d, J = 8.0), 8.48 (1H, d, J = 8.4), 8.60 (1H, m), 8.78 (1H, d, J = 8.4), 9.29 (1H, d), 9.42 (1H, d), 9.64 (1H, s). QTOF-MS ES^+ (Figure S5), m/z $(M+H)^+$, calculated for $C_{23}H_{16}N$: 306.3875, found: 306.3. FTIR (neat) (Figure S6) ν_{max} = 1577 cm^{-1}.

Synthesis of 2-(benzylideneamino) benzoic acid (ANB) (Scheme 1)

ANB has been prepared with 70% yield by conjugating anthranilic acid (0.05 g, 0.365 mmol) with benzaldehyde (0.039 g, 0.365 mmol) in methanol. A dark brown product obtained was recrystallized from methanol. The product was characterized by: ^{1}H NMR (Figure S7) (400 MHz, DMSO-d_6) δ (ppm): 6.51 (2H, m), 6.73 (2H, m), 7.23 (2H, d, J = 8.4), 7.60 (1H, d, J = 7.6), 7.78 (2H, d, J = 6.8), 7.95 (1H, t, J = 6.8). QTOF-MS ES^+ (Figure S8), m/z $(M+H)^+$, calculated for $C_{14}H_{12}NO_2$: 226.0863, found: 226.1155. FTIR (neat) (Figure S9) ν_{max} = 1586, 1611 and 1650 cm^{-1}.

Results and discussion

Among three probes, two have been prepared by condensation of pyrene-1-carboxaldehyde with anthranilic acid (**ANP**) and aniline (**APA**), while the third one involves condensation of benzaldehyde with anthranilic acid (**ANB**) (Scheme 1). The probes are characterized by ^{1}H NMR, QTOF-mass and FTIR spectra (Figures S1–S9, Electronic Supplementary Information (ESI)). **ANP**, **APA** and **ANB** have absorbance at 360, 365 and 335 nm, respectively (Figure 1), allowing as FRET acceptor for naphthalene (λ_{em}, 335 nm; λ_{ex}, 280 nm). Increasing naphthalene concentration to the solution having fixed amount of ANB, APA and ANP enhance their emission intensities, indicating FRET process. Weak emission of ANB (λ_{em}, 420 nm; 20 μM, Figure 2) gradually enhances on concomitant addition of naphthalene (0.1–10 μM), attributed to FRET from naphthalene to ANB. Interestingly, addition of naphthalene over 10 μM does not alter the overlap area with no further change of emission intensity. Reverse titration, where gradual addition of ANB to fixed amount of naphthalene (Figure S10, ESI) quenches naphthalene fluorescence because of energy transfer from naphthalene to **ANB**. Plots of emission intensities versus concentrations of naphthalene and **ANB** generate two sigmoidal curves, the first one being growth (Figure S11, ESI), and the later one is decay curve (Figure S12, ESI).

On the other hand, **APA** (λ_{em}, 459 nm, λ_{ex}, 280 nm) also participates in the FRET process with naphthalene as reflected by its fluorescence enhancement with increasing naphthalene content. However, LOD of **APA** for naphthalene is lower than that of **ANB**. It can detect as low as 1.0 μM naphthalene (Figure 3). Plot of emission intensity of **APA** as a function of naphthalene concentration is sigmoidal (Figure S13, ESI). Reverse titration by gradual addition of **APA** to a fixed amount

Journal of Molecular Recognition

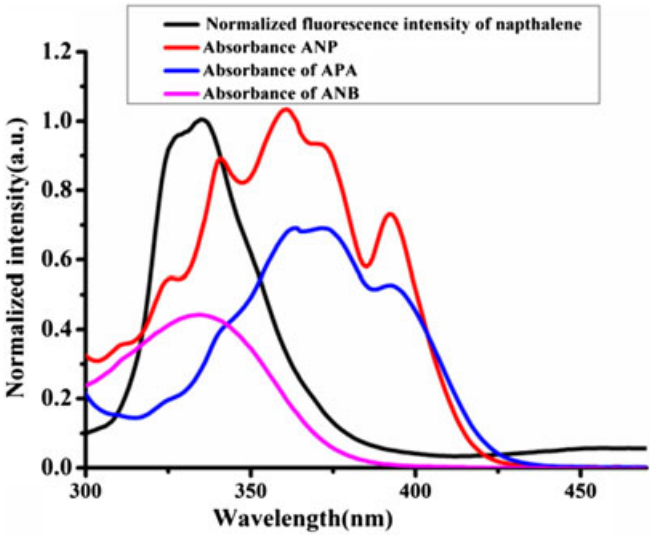

Figure 1. Overlap of emission of the donor (naphthalene, 50 μM) and absorption of acceptors (**ANP**, **APA** and **ANB**, 20 μM) in methanol : water (4:1, v/v).

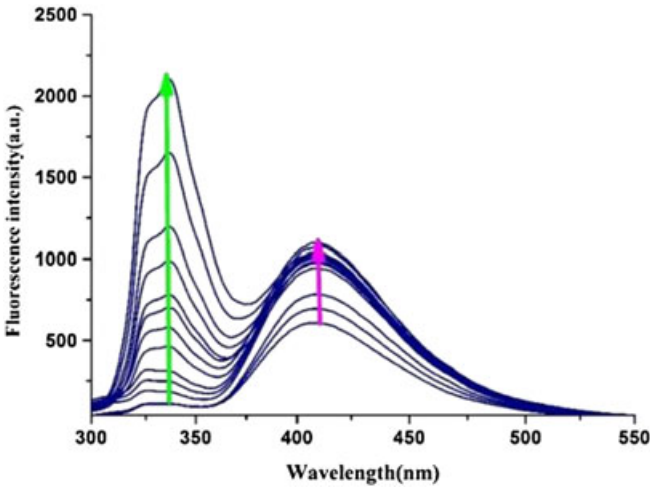

Figure 2. Changes in the emission spectra of **ANB** (20 μM, λ_{ex}, 280 nm) in methanol : water (4:1, v/v) upon gradual addition of naphthalene (0, 0.1, 0.5, 1.0, 2.0, 3.0, 5.0, 10.0, 15.0, 20.0, 30.0, 50.0, 75.0 and 100.0 μM).

of naphthalene (Figure S14, ESI) corroborates the said FRET process. A sigmoidal decay curve is obtained when fluorescence intensity of naphthalene (50 μM) is plotted against **APA** concentration (Figure S15, ESI).

Focusing to enhance the LOD for naphthalene, tuning of FRET efficiency is necessary (overlap area of naphthalene donor emission and absorbance of probe acceptor). LOD of **ANP** (λ_{em}, 459 nm; λ_{ex}, 280 nm) for naphthalene is 0.01 μM. Because of the presence of pyrene unit, it has higher absorbance at longer wavelength than that of **ANB** (Figure 1), thus enabling larger overlap area between naphthalene emission and **ANP** absorbance at higher naphthalene concentration (up to 1000 μM). Figure 4 shows the fluorescence enhancement of **ANP** upon gradual addition of naphthalene (from 0.01 μM to 1000.0 μM), while Figure S16 (ESI) shows the related sigmoidal curve. Figure S15 (ESI) has two linear regions, viz. 0.1 to 5 μM and 5 to 30 μM (Figure 5), useful for determination of unknown naphthalene

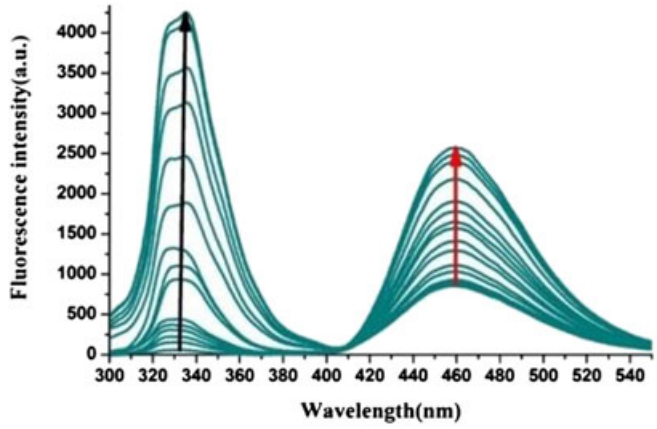

Figure 3. Changes in the emission spectra of **APA** (20 μM, λ_{ex}, 280 nm) upon gradual addition of naphthalene (0, 1.0, 2.0, 3.0, 5.0, 10.0, 15.0, 20.0, 30.0, 50.0, 75.0, 100.0, 200.0, 500.0 and 1000.0 μM) in methanol–water (4:1, v/v).

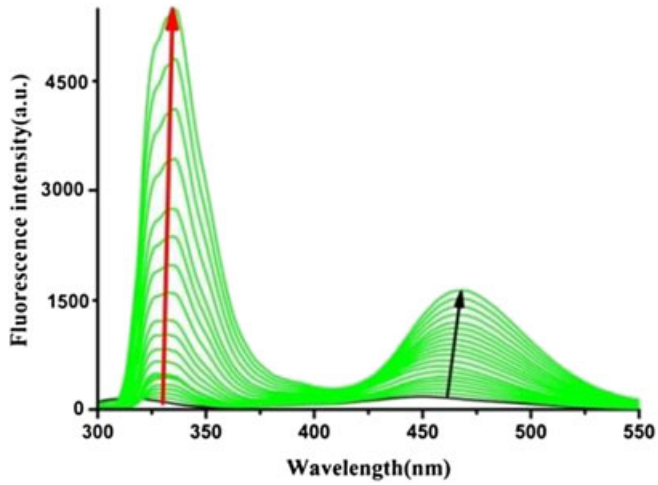

Figure 4. Changes in the emission spectra of **ANP** (20 μM, λ_{ex}, 280 nm) in methanol–water (4:1, v/v) upon gradual addition of naphthalene (0, 0.01, 0.05, 0.1, 0.5, 1.0, 2.0, 3.0, 5.0, 10.0, 15.0, 20.0, 30.0, 50.0, 75.0, 100.0, 200.0, 300.0, 500.0 and 1000.0 μM).

concentration. Reverse fluorescence titration for **ANP** (Figure 6) shows quenching of naphthalene fluorescence upon increasing **ANP** concentration, while Figure S17 (ESI) reveals the corresponding hyperbolic decay curve. The quenching of naphthalene fluorescence is highest for **ANP** compared with **ANB** and **APA**.

Förster distances (R_o) between donor and acceptor in all three cases have been calculated using the equation (Lakowicz, 2006), $R_o = 0.2108\ [K^2 \Phi_o\ n^{-4} J]^{1/6}$. The values of R_o for **ANP**, **APA** and **ANB** are 27.77, 25.11 and 24.24 Å, respectively (Table S1, ESI). Moreover, with decreasing (r/R_o),that is, with increasing R_o, energy transfer efficiency (E) increases. If it is assumed that the real distance (r) between naphthalene and all three probes remain the same, **ANP** will show the highest energy transfer efficiency. Efficiency of energy transfer from naphthalene to the probes has also been calculated using the equation ((Lakowicz), $\mathbf{E = 1 - (F_{DA}/F_D)}$ where F_{DA} and F_D represent emission intensities of donor in presence and absence of acceptor, respectively. The calculated values in presence of naphthalene (1000.0 μM) are 0.860, 0.791 and 0.772 **ANP**, **APA** and **ANB** (20 μM), respectively.

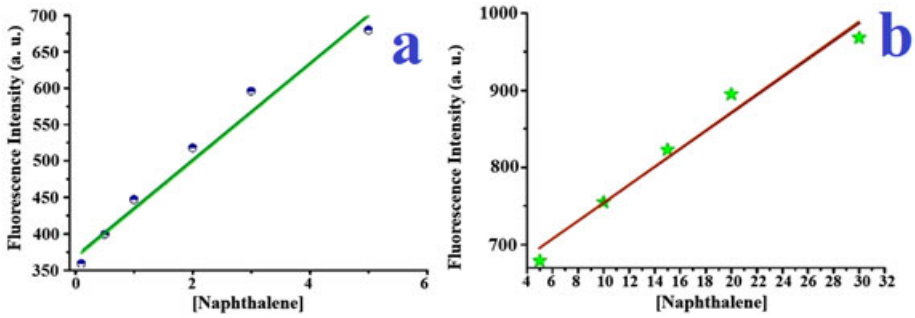

Figure 5. Linear plots: (a) 0.1 to 5 μM and (b) 5 to 30 μM of added naphthalene.

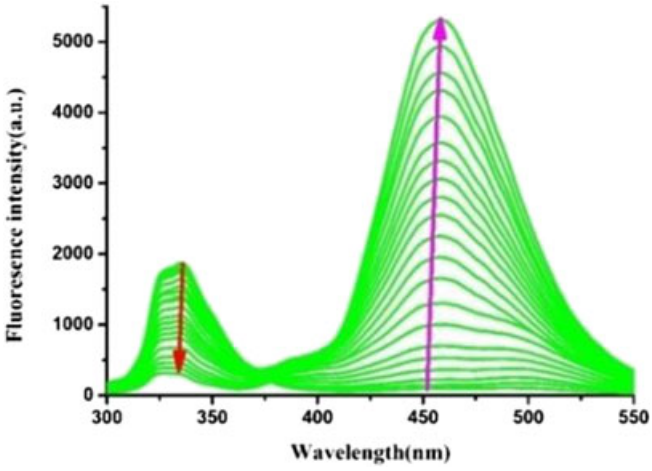

Figure 6. Changes of the emission spectra of naphthalene (50 μM, λ_{ex} = 280 nm) upon gradual addition of **ANP** (0, 0.01, 0.05, 0.1, 0.5, 1.0, 2.0, 3.0, 5.0, 10.0, 15.0, 20.0, 30.0, 50.0, 75.0, 100.0, 200.0, 300.0, 400.0, 500.0 and 1000.0 μM).

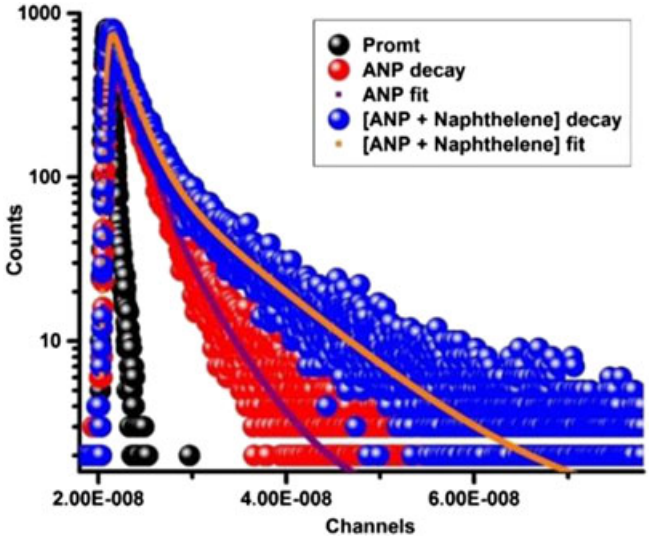

Figure 7. Fluorescence lifetime decay of **ANP** (20 μM) and the (**ANP** + naphthalene) systems in methanol : water (4:1, v/v) medium (λ_{ex}, 280 nm and λ_{em}, 459 nm).

Figure 1 clearly shows the higher overlap integral between naphthalene emission (donor) and **ANP** absorption than that of **ANB** and **APA**, indicating stronger FRET process involving **ANP**. This allows **ANP** to detect much lower naphthalene concentration. Among most of the PAHs, only naphthalene may act as an effective FRET donor for all the three probes. Naphthalene having 335 nm emission is an ideal candidate for overlap with the absorption of **ANB** (335 nm), **APA** (365 nm) and **ANP** (360 nm), which is absent for other PAHs like dibenzo(a,h)anthracene (λ_{em}, 404 nm), benzo(ghi)perylene (λ_{em}, 394 nm), indigo (1,2,3 cd)pyrene (λ_{em}, 496 nm), benzo(a)pyrene (λ_{em}, 406 nm), benzo(b) fluoranthene (λ_{em}, 446 nm), crycene (λ_{em}, 386 nm), benzo(k)fluoranthene (λ_{em}, 414 nm), pyrene (λ_{em}, 406 nm), fluoranthrene (λ_{em}, 460 nm) and anthracene (λ_{em}, 402 nm) (Fernández-Sánchez *et al*., 2003)

However, **APA** and **ANP** have insignificant overlap with benzo (ghi)perylene and crycene compared with naphthalene; however, they do not have excitation near 280 nm. Thus, the earlier discussion clearly demonstrates that **ANB**, **APA** and **ANP** are suitable for selective determination of naphthalene.

In presence of naphthalene, the fluorescence lifetime of **ANP** (at 459 nm, acceptor emission) increases to 3.07 ns from that of free **ANP** (2.23 ns), supporting the FRET process (Figure 7). Common cations (Li^+, Na^+, K^+, Ag^+, Cd^{2+}, Mg^{2+}, Zn^{2+}, Ca^{2+}, Pb^{2+}, Co^{2+}, Hg^{2+} and Cu^{2+}) and anions (F^-, Cl^-, Br^-, I^-, AcO^-, N_3^-, SCN^-, ClO_4^-, NO_3^-, SO_4^{2-} and $H_2PO_4^-$) normally present in water do not show any significant interference (Figures S18 and S19).

Application

Gomati River, a tributary of the River Ganga, is one of the most polluted rivers in India is affected during its course by three major urban centers, viz. Lucknow, Sultanpur and Jaunpur. Several groups are working to measure the concentration of PAHs in this water. The developed method is used to determine the contamination of naphthalene in the Gomati river water. The method is also used to determine percent recovery of naphthalene in Mili-Q water. To evaluate the accuracy of the method, recovery studies have been performed at different concentration levels of naphthalene. Standard addition method is used for determination of naphthalene in water (Ellison and Thompson, 2008). Results obtained are summarized in Tables S2 and S3 for Mili-Q and river water, respectively. Table S3 indicates close resemblance of the present results to that obtained using high-performance liquid chromatography method (Malik *et al*., 2011), indicating the efficiency of **ANP** for naphthalene determination.

Journal of Molecular Recognition

CONCLUSION

Three new low-cost fluorescence probes, viz. **ANB**, **APA** and **ANP**, participate in the FRET process with naphthalene. FRET efficiency is highest for **ANP** that allows lowest LOD for naphthalene. Fluorescence lifetime data support the FRET process. Finally, **ANP** has been successfully used to determine naphthalene concentration of Gomti river water, first time ever.

Acknowledgements

Authors sincerely thank the Department of Environment, Govt. of West Bengal for financial support. S. Nandi gratefully acknowledges UGC for fellowship. Authors thank Dr. Bankim Chandra Ghosh Haldia Government College, West Bengal, India, for his help.

REFERENCES

Agency for Toxic Substances and Disease Registry (ATSDR). 1996. Toxicological profile for naphthalene. U. S. Department of Health and Human Services: Atlanta, GA.

Anbu, S, Shanmugaraju, S, Ravishankaran, R, Karande, AA, Mukherjee, PS. 2012. Naphthylhydrazone based selective and sensitive chemosensors for Cu^{2+} and their application in bioimaging. *Dalton Trans.* **41**: 13330–13337.

Andreoli, R, Manini, P, Bergamaschi, E, Mutti, A, Franchini, I, Niessen, WMA. 1999. Determination of naphthalene metabolites in human urine by liquid chromatography–mass spectrometry with electrospray ionization. *J. Chromatogr. A* **847**: 9–17.

Aoki, I, Sakaki, T, Shinkai, SJ. 1992. A new metal sensory system based on intramolecular fluorescence quenching on the ionophoriccalix[4]arene ring. *J. Chem. Soc., Chem. Commun.* 730–732.

Banerjee, A, Sahana, A, Guha, S, Lohar, S, Hauli, I, Mukhopadhyay, SK, Matalobos, JS, Das, D. 2012. Nickel(II)-induced excimer formation of a naphthalene-based fluorescent probe for living cell imaging. *Inorg. Chem.* **51**: 5699–5704.

Banerjee, A, Sahana, A, Lohar, S, Hauli, I, Mukhopadhyay, SK, Safin, DA, Babashkina, MG, Bolte M, Garcia Y, Das, D. 2013a. A rhodamine derivative as a "lock" and SCN – as a "key": visible light excitable SCN− sensing in living cells. *Chem. Commun.* **49**: 2527–2529.

Banerjee, A, Sahana, A, Lohar, S, Sarkar, B, Mukhopadhyay, SK, Das, D. 2013b. A FRET operated sensor for intracellular pH mapping: strategically improved efficiency on moving from an anthracene to a naphthalene derivative. *RSC Adv.* **3**: 14397–14405.

Das, S, Guha, S, Banerjee, A, Lohar, S, Sahana, A, Das, D. 2011. 2-(2-Pyridyl) benzimidazole based Co(II) complex as an efficient fluorescent probe for trace level determination of aspartic and glutamic acid in aqueous solution: a displacement approach. *Org. Biomol. Chem.* **9**: 7097–7104.

Das, S, Sahana, A, Banerjee, A, Lohar, S, Guha, S, Matalobos, JS, Das, D. 2012. Thiophene anchored naphthalene derivative: Cr^{3+} selective turn-on fluorescent probe for living cell imaging. *Anal. Methods* **4**: 2254–2258.

Das, S, Sahana, A, Banerjee, A, Lohar, S, Safin, DA, Babashkina, MG, Bolte, M, Garcia, Y, Hauli, I, Mukhopadhyay, SK, Das, D. 2013. Ratiometric fluorescence sensing and intracellular imaging of Al^{3+} ions driven by an intramolecular excimer formation of a pyrimidine–pyrene scaffold. *Dalton Trans.* **42**: 4757–4763.

Diaz, RC, Sarasa, MA, Rios, C, Cuello, JJ. 1999. Validation of an HPLC method for the determination of p-dichlorobenzene and naphthalene in moth repellents. *Accredit. Qual. Assur.* **4**: 473–476.

Ellison, SLR, Thompson, M. 2008. Standard additions: myth and reality. *Analyst* **133**: 992–997.

Fernández-Sánchez, JF, Carretero, AS, Cruces-Blanco, C, Fernández-Gutiérrez, A. 2003. The development of solid-surface fluorescence characterization of polycyclic aromatic hydrocarbons for potential screening tests in environmental samples. *Talanta* **60**: 287–293.

Förster, T. 1948. Intermolecular energy migration and fluorescence. *Ann. Phys.* **2**: 55–75.

Förster, T. 1949. Experimentelle and theoretische Untersuchung des zwischenmolekularen Übergangs von Elektronenanregungsenergie. *Z. Naturforsch. A: Astrophys. Phys. Phys. Chem.* **4**: 321–327.

Gautam, R, Srivastava, A, Jachak, SM. 2011. Simultaneous determination of naphthalene and anthraquinone derivatives in Rumex nepalensis Spreng. Roots by HPLC: comparison of different extraction methods and validation. *Phytochem. Anal.* **22**: 153–157.

Guha, S, Lohar, S, Banerjee, A, Sahana, A, Chaterjee, A, Mukherjee, SK, Matalobos, JS, Das, D. 2012. Thiophene anchored coumarin derivative as a turn-on fluorescent probe for Cr^{3+}: cell imaging and speciation studies. *Talanta* **91**: 18–25.

Han, TY, Feng, X, Tong, B, Shi, JB, Chen, L, Zhi, JG, Dong, YP. 2012. A novel "turn-on" fluorescent chemosensor for the selective detection of Al^{3+} based on aggregation-induced emission. *Chem. Commun.* **48**: 416–418.

Hossain, MA, Yeasmin, F, Rahman, SMM, Rana, MS. 2014. Naphthalene, a polycyclic aromatic hydrocarbon, in the fish samples from the Bangsai river of Bangladesh by gas chromatograph–mass spectrometry. *Arabian J. Chem.* **7**: 976–980.

Ji, HF, Brown, GM, Dabestani, R. 1999. Calix[4]arene-based Cs^{+} selective optical sensor. *Chem. Commun.* 609–610.

Kim, JS, Quang, DT. 2007. Calixarene derived fluorescent probes. *Chem. Rev.* **107**: 3780–3799.

Kishikawa, N, Wada, M, Kuroda, N, Akiyama, S, Nakashima, K. 2003. Determination of polycyclic aromatic hydrocarbons in milk samples by high-performance liquid chromatography with fluorescence detection. *J. Chromatogr. B* **789**: 257–264.

Lakowicz, JR. 2006. Principles of fluorescence spectroscopy. University of Maryland School of Medicine Baltimore: Maryland, USA.

Leray, I, Lefevre, JP, Delouis, JF, Delaire, J, Valeur, B. 2001. Synthesis and photophysical and cation-binding properties of mono- and tetranaphthylcalix[4]arenes as highly sensitive and selective fluorescent sensors for sodium. *Chem. Eur. J.* **7**: 4590–4598.

Leray, I, Reilly, FO, HabibJiwan, JL, Soumillion, JP, Valeur, BA. 1999. A new calix[4]arene-based fluorescent sensor for sodium ion. *Chem. Commun.* 795–796.

Lim, NC, Schuster, JV, Porto, MC, Tanudra, MA, Yao, L, Freake, HC, Bruckner, C. 2005. Coumarin-based chemosensors for zinc(II): toward the determination of the design algorithm for CHEF-type and ratiometric probes. *Inorg. Chem.* **44**: 2018–2030.

Lohar, S, Sahana, A, Banerjee, A, Banik, A, Mukhopadhyay, SK, Matalobos, JS, Das, D. 2013. Antipyrine based arsenate selective fluorescent probe for living cell imaging. *Anal. Chem.* **85**: 1778–1783.

Malik, A, Verma, P, Singh, AK, Singh, KP. 2011. Distribution of polycyclic aromatic hydrocarbons in water and bed sediments of the Gomti River, India. *Environ. Monit. Assess.* **172**: 529–545.

Sahana, A, Banerjee, A, Das, S, Lohar, S, Karak, D, Sarkar, B, Mukhopadhyay, SK, Mukherjee, AK, Das, D. 2011. A naphthalene-based Al^{3+} selective fluorescent sensor for living cell imaging. *Org. Biomol. Chem.* **9**: 5523–5529.

Sahana, A, Banerjee, A, Guha, S, Lohar, S, Chattopadhyay, A, Mukhopadhyay, SK, Das, D. 2012. Highly selective organic fluorescent probe for azide ion: formation of a "molecular ring". *Analyst* **137**: 1544–1546.

Serio, N, Miller, K, Levine, M. 2013. Efficient detection of polycyclic aromatic hydrocarbons and polychlorinated biphenyls *via* three-component energy transfer. *Chem. Commun.* **49**: 4821–4823.

U.S. Environmental Protection Agency. 1994. Health effects notebook for hazardous air pollutants. Office of Air Planning & Standards: Naphthalene.

Van Der Meer, BW, Coker, GI, Simon Chen, S-Y. 1994. Resonance energy transfer: theory and data. VCH: New York.

Wang, JB, Qian, XF, Cui, JN. 2006. Detecting Hg^{2+} ions with an ICT fluorescent sensor molecule: remarkable emission spectra shift and unique selectivity. *J. Org. Chem.* **71**: 4308–4311.

Weller, A. 1956. Intramolecular proton transfer in excited states. *Zeitscrift für Elektrochemie* **60**: 1144–1147.

Xu, Z, Xiao, Y, Qian, X, Cui, J, Cui, D. 2005. Ratiometric and selective fluorescent sensor for Cull based on internal charge transfer (ICT). *Org. Lett.* **7**: 889–892.

Zhu, JW, Qin, Y, Zhang, YH. 2010. Magnesium-selective ion-channel mimetic sensor with a traditional calcium ionophore. *Anal. Chem.* **82**: 436–440.

SUPPORTING INFORMATION

Additional supporting information can be found in the online version of this article at the publisher's website.

